



Published in final edited form as:

Science. 2014 July 25; 345(6195): 437–440. doi:10.1126/science.1255525.

Merging photoredox with nickel catalysis: Coupling of α -carboxyl sp^3 -carbons with aryl halides

Zhiwei Zuo, Derek T. Ahneman, Lingling Chu, Jack A. Terrett, Abigail G. Doyle^{*}, and David W. C. MacMillan^{*}

Merck Center for Catalysis at Princeton University, Princeton, NJ 08544, USA

Abstract

Over the past 40 years, transition metal catalysis has enabled bond formation between aryl and olefinic (sp^2) carbons in a selective and predictable manner with high functional group tolerance. Couplings involving alkyl (sp^3) carbons have proven more challenging. Here, we demonstrate that the synergistic combination of photoredox catalysis and nickel catalysis provides an alternative cross-coupling paradigm, in which simple and readily available organic molecules can be systematically used as coupling partners. By using this photoredox-metal catalysis approach, we have achieved a direct decarboxylative sp^3 – sp^2 cross-coupling of amino acids, as well as α -O- or phenyl-substituted carboxylic acids, with aryl halides. Moreover, this mode of catalysis can be applied to direct cross-coupling of C_{sp^3} -H in dimethylaniline with aryl halides via C–H functionalization.

Visible light photoredox catalysis has emerged in recent years as a powerful technique in organic synthesis. This class of catalysis makes use of transition metal polypyridyl complexes that, upon excitation by visible light, engage in single-electron transfer (SET) with common functional groups, activating organic molecules toward a diverse array of valuable transformations (1–5). Much of the utility of photoredox catalysis hinges on its capacity to generate nontraditional sites of reactivity on common substrates via low-barrier, open-shell processes, thereby fostering the use of abundant and inexpensive starting materials.

Over the past century, transition metal-catalyzed cross-coupling reactions have evolved to be among the most used C–C and C–heteroatom bond-forming reactions in chemical synthesis. In particular, nickel catalysis has provided numerous avenues to forge carbon–carbon bonds via a variety of well-known coupling protocols (Negishi, Suzuki-Miyaura, Stille, Kumada, and Hiyama couplings, among others) (6, 7). The broad functional group tolerance of these reactions enables a highly modular building block approach to molecule

^{*}Corresponding author. agdoyle@princeton.edu (A.G.D.); dmacmill@princeton.edu (D.W.C.M.).

SUPPLEMENTARY MATERIALS

www.sciencemag.org/content/345/6195/437/suppl/DC1

Material and Methods

Supplementary Text

Tables S1 and S2

Data

References (26–34)

construction. Organometallic cross-coupling methods are traditionally predicated on the use of aryl or vinyl boronic acids, zinc halides, stannanes, or Grignard fragments that undergo addition to a corresponding aryl or vinyl halide partner.

We recently questioned whether visible-light photoredox and nickel transition metal catalysis might be successfully combined to create a dual catalysis platform for modular C–C bond formation (Fig. 1) (8–14). Through a synergistic merger of these two activation modes, we hoped to deliver a mechanism by which feedstock chemicals that contain common yet nontraditional leaving groups (C_{sp^3} –CO₂H or C_{sp^3} –H bonds) could serve as useful coupling partners. Among many advantages, this multicatalysis strategy would enable a modular approach to sp^3 – sp^2 or sp^3 – sp^3 bond formations that is not currently possible by using either photoredox or transition metal catalysis alone. We sought to develop a general method that would exploit naturally abundant, inexpensive, and orthogonal functional handles (e.g., C–CO₂H, C–H with C–Br, or C–I).

We proposed that two interwoven catalytic cycles might be engineered to simultaneously generate (i) an organometallic nickel(II) species via the oxidative addition of a Ni(0) catalyst to an aryl (Ar), alkenyl, or alkyl halide coupling partner and (ii) a carbon-centered radical generated through a photomediated oxidation event (Fig. 2). Given that organic radicals are known to rapidly combine with Ni(II) complexes (15, 16), we hoped that this dual catalysis mechanism would successfully converge in the form of Ni(III)(Ar)(alkyl) that, upon reductive elimination, would deliver our desired C–C fragment coupling product. One of our laboratories has demonstrated that photoredox catalysis affords access to α -amino radicals by two distinct methods: via decarboxylation of a carboxylic acid or by an oxidation, deprotonation sequence with *N*-aryl or trialkyl amines (17, 18). The other laboratory has explored Ni-catalyzed cross-coupling reactions with iminium ions that proceed via a putative α -aminonickel intermediate (19–21). Given our respective research areas, we sought to jointly explore the capacity of a nickel (II) aryl species to intercept a photoredox-generated α -amino radical, thereby setting the stage for the fragment coupling. We recognized that the sum of these two catalytic processes could potentially overcome a series of limitations that exist for each of these catalysis methods in their own right.

A detailed description of our proposed mechanistic cycle for the decarboxylative coupling is outlined in Fig. 2. We presumed that initial irradiation of heteroleptic iridium(III) photocatalyst Ir[dF(CF₃)ppy]₂(dtbbpy)PF₆ [dF(CF₃)ppy = 2-(2,4-difluorophenyl)-5-(trifluoromethyl)pyridine, dtbbpy = 4,4'-di-*tert*-butyl-2,2'-bipyridine] (**1**) would produce the long-lived photoexcited *Ir^{III} state **2** (exposure time τ = 2.3 μ s) (**22**). Deprotonation of the α -amino acid substrate **3** with base and oxidation by the excited-state *Ir^{III} complex { $E_{1/2}^{red}$ [*Ir^{III}/Ir^{II}] = +1.21 V versus saturated calomel electrode (SCE) in CH₃CN} (**22**) via a SET event would then generate a carboxyl radical, which upon rapid loss of CO₂ would deliver the α -amino radical **4** and the corresponding Ir^{II} species **5**. Given the established oxidation potential of prototypical amino acid carboxylate salts, we expected this process to be thermodynamically favorable [*tert*-butyl carbamoyl (Boc)–Pro–OCs, $E_{1/2}^{red}$ = +0.95 V versus SCE in CH₃CN) (17). Concurrently with this photoredox cycle, we hoped that oxidative addition of the Ni(0) species **6** into an aryl halide would produce the Ni(II) intermediate **7**. We anticipated that this Ni(II)-aryl species would rapidly intercept the α -

amino radical **4**, forming the organometallic Ni(III) adduct **8**. Subsequent reductive elimination would forge the requisite C–C bond while delivering the desired α -amino arylation product **10** and expelling the Ni(I) intermediate **9**. Last, SET between the Ir^{II} species **5** and the Ni complex **9** would accomplish the exergonic reduction of Ni(I) to Ni(0) {on the basis of the established two-electron reduction potential of Ni(II) to Ni(0), we presume that reduction of Ni(I) to Ni(0) should be thermodynamically favorable, $E_{1/2}^{\text{red}}[\text{Ni}^{\text{II}}/\text{Ni}^0] = -1.2$ V versus SCE in *N,N'*-dimethylformamide (DMF)} by the Ir^{II} species **5** { $E_{1/2}^{\text{red}}[\text{Ir}^{\text{III}}/\text{Ir}^{\text{II}}] = -1.37$ V versus SCE in CH₃CN} (22, 23), thereby completing both the photoredox and the nickel catalytic cycles simultaneously.

With this mechanistic hypothesis in hand, we first examined the proposed coupling by using *N*-Boc proline, *para*-iodotoluene, and a wide range of photoredox and ligated nickel catalysts. To our delight, we found that the combination of Ir[dF(CF₃)ppy]₂(dtbbpy)PF₆ and NiCl₂•glyme (glycol ether), dtbbpy, in the presence of 1.5 equivalents of Cs₂CO₃ base and white light from a 26-W compact fluorescent bulb, achieved the desired fragment coupling in 78% yield. During our optimization studies, we found that use of a bench-stable Ni(II) source, such as NiCl₂•glyme, was sufficient to generate the arylation product with comparable efficiency to a Ni(0) source. We attribute this result to in situ photocatalytic reduction of Ni(II) to Ni(0) via two discrete SET events, with excess amino acid likely serving as the sacrificial reductant to access the active Ni catalyst { $E_{1/2}^{\text{red}}[\text{Ni}^{\text{II}}/\text{Ni}^0] = -1.2$ V versus SCE in DMF} (23). We believe that it is unlikely that the Ni(II)(Ar) X intermediate **7** undergoes a SET event to form Ni(I)Ar, given the poorly matched reduction potentials of the species involved {compare with $E_{1/2}^{\text{red}}[\text{Ni}^{\text{II}}\text{ArX}/\text{Ni}^{\text{I}}\text{Ar}] = -1.7$ V versus SCE in CH₃CN and $E_{1/2}^{\text{red}}[\text{Ir}^{\text{III}}/\text{Ir}^{\text{II}}] = -1.37$ V versus SCE in CH₃CN} (22, 24). However, we recognize that an alternative pathway could be operable wherein the oxidative addition step occurs from the Ni(I) complex to form a Ni(III) aryl halide adduct. In this pathway, photocatalyst-mediated reduction of the aryl-Ni(III) salt to the corresponding Ni(II) species followed by the α -amino radical addition step would then form the same productive Ni(III) adduct **8**, as shown in Fig. 2. Given that (i) Ni(0) complexes undergo oxidative addition more readily than Ni(I) complexes with aryl halides (25) and (ii) Ni(II) complexes are believed to rapidly engage with sp³ carbon-centered radicals to form Ni(III) species (enabling sp³–sp² and sp³–sp³ C–C bond formations) (15, 16), we favor the dual-catalysis mechanism outlined in Fig. 2.

Having established the optimal conditions for this photoredox-nickel decarboxylative arylation, we focused our attention on the scope of the aryl halide fragment. As shown in Fig. 3, a wide range of aryl iodides are amenable to this dual-catalysis strategy, including both electron-rich and electron-deficient arenes (**10** to **13**, 65 to 78% yield). Many aryl bromides function effectively as well, including those that contain functional groups as diverse as ketones, esters, nitriles, trifluoromethyl groups, and fluorides (**14** to **18**, 75 to 90% yield). Heteroaromatics, in the form of differentially substituted bromopyridines, are also efficient coupling partners (**19** to **22**, 60 to 85% yield). Moreover, aryl chlorides are competent substrates if the arenes, such as pyridines and pyrimidines, are electron-deficient (**23** and **24**, 64 and 65% yield). Only products **15** and **19** in Fig. 3 would be accessible by using our previously reported photoredox arylation strategy. Moreover, we are unaware of

the general use of C_{sp}³-bearing carboxylic acids as reaction substrates in transition metal catalysis, an illustration of the tremendous scope expansion that is attainable by using this dual catalysis technology. These reactions are typically complete in 72 hours at larger scale and 48 hours on smaller scale (see supplementary text).

Next, we investigated the nature of the carboxylic acid coupling partner, as highlighted in Fig. 4A. A wide variety of α -amino acids function effectively in this protocol, including various *N*-Boc and *N*-benzyl carbamoyl (*N*-Cbz) protected heterocycles (**25** to **27**, 61 to 93% yield). Acyclic α -amino acids, containing indole, ester, and thioether functionalities, are also readily tolerated (**28** to **32**, 72 to 91% yield). α -oxycarboxylic acids can function as proficient coupling partners, producing α -arylated ethers in high yield over a single step (**33**, 82% yield). Moreover, we have also found that various phenyl acetic acid substrates function in this coupling protocol with high efficiency (>78% yield, see supplementary text).

To further demonstrate the utility of this dual-catalysis strategy, we sought to demonstrate the direct functionalization of C_{sp}³-H bonds with coupling partners derived from aryl or alkyl halides. Given that our decarboxylation-arylation mechanism involves the rapid addition of an α -amino radical to a Ni(II) salt, we sought to generate an analogous α -nitrogen carbon-centered radical via a photoredox-driven *N*-phenyl (*N*-Ph) oxidation, α -C-H deprotonation sequence using aniline-based substrates (**18**). We presumed that this photomediated *N*-Ph oxidation mechanism would provide an alternative pathway to the open-shell carbon intermediate (corresponding to **4**, Fig. 2) and should similarly intercept the putative Ni(II) intermediate **8**. Assuming that the remaining dual-catalysis mechanism would be analogous to that shown in Fig. 2, we expected that a range of direct C_{sp}³-H functionalization protocols should be possible. Indeed, we were able to demonstrate that dimethylaniline undergoes α -amine coupling with a variety of aryl halides in the presence of Ir[dF(CF₃)ppy]₂(dtbbpy)PF₆ and NiCl₂•glyme (Fig. 4B). Electron-deficient and electron-rich iodoarenes give moderate to high yields (**34** to **36**, 72 to 93% yield). Moreover, aryl bromides are competent coupling partners, enabling the installation of medicinally important heterocyclic motifs (**37**, 60% yield). Last, control experiments have revealed that the combination of light, photoredox catalyst **1**, and the NiCl₂•dtbbpy complex is essential for product formation in all examples listed in Figs. 3 and 4. This reaction represents a powerful foray into direct C-H activation using orthogonal cross-coupling reactivity.

Supplementary Material

Refer to Web version on PubMed Central for supplementary material.

ACKNOWLEDGMENTS

The authors are grateful for financial support provided by the NIH General Medical Sciences (grants NIHGM5 R01 GM103558-01 and R01 GM100985-01) and gifts from Merck, Amgen, Eli Lilly, and Roche. Z.Z. and L.C. are grateful for postdoctoral fellowships from the Shanghai Institute of Organic Chemistry. The authors thank G. Molander and co-workers for graciously offering to concurrently publish a related study that was submitted slightly ahead of our own.

REFERENCES AND NOTES

1. Nicewicz DA, MacMillan DWC. *Science*. 2008; 322:77–80. [PubMed: 18772399]
2. Ischay MA, Anzovino ME, Du J, Yoon TP. *J. Am. Chem. Soc.* 2008; 130:12886–12887. [PubMed: 18767798]
3. Narayanam JMR, Tucker JW, Stephenson CRJ. *J. Am. Chem. Soc.* 2009; 131:8756–8757. [PubMed: 19552447]
4. Hamilton DS, Nicewicz DA. *J. Am. Chem. Soc.* 2012; 134:18577–18580. [PubMed: 23113557]
5. Pirnot MT, Rankic DA, Martin DBC, MacMillan DWC. *Science*. 2013; 339:1593–1596. [PubMed: 23539600]
6. Netherton MR, Fu GC. *Adv. Synth. Catal.* 2004; 346:1525–1532.
7. Rudolph A, Lautens M. *Angew. Chem. Int. Ed.* 2009; 48:2656–2670.
8. The successful merger of photoredox and transition metal catalysis has been demonstrated for the specific installation of unique functionality (e.g., CF₃) (*9–14*).
9. Osawa M, Nagai H, Akita M. *Dalton Trans.* 2007; 2007:827–829. [PubMed: 17297509]
10. Kalyani D, McMurtrey KB, Neufeldt SR, Sanford MS. *J. Am. Chem. Soc.* 2011; 133:18566–18569. [PubMed: 22047138]
11. Ye Y, Sanford MS. *J. Am. Chem. Soc.* 2012; 134:9034–9037. [PubMed: 22624669]
12. Rueping M, et al. *Chemistry*. 2012; 18:5170–5174. [PubMed: 22431393]
13. Sahoo B, Hopkinson MN, Glorius F. *J. Am. Chem. Soc.* 2013; 135:5505–5508. [PubMed: 23565980]
14. Shu XZ, Zhang M, He Y, Frei H, Toste FD. *J. Am. Chem. Soc.* 2014; 136:5844–5847. [PubMed: 24730447]
15. Biswas S, Weix DJ. *J. Am. Chem. Soc.* 2013; 135:16192–16197. [PubMed: 23952217]
16. Zultanski SL, Fu GC. *J. Am. Chem. Soc.* 2013; 135:624–627. [PubMed: 23281960]
17. Zuo Z, MacMillan DWC. *J. Am. Chem. Soc.* 2014; 136:5257–5260. [PubMed: 24712922]
18. McNally A, Prier CK, MacMillan DWC. *Science*. 2011; 334:1114–1117. [PubMed: 22116882]
19. Graham TJA, Shields JD, Doyle AG. *Chem. Sci.* 2011; 2:980.
20. Sylvester KT, Wu K, Doyle AG. *J. Am. Chem. Soc.* 2012; 134:16967–16970. [PubMed: 23030789]
21. Shields JD, Ahneman DT, Graham TJA, Doyle AG. *Org. Lett.* 2014; 16:142–145. [PubMed: 24279380]
22. Lowry MS, et al. *Chem. Mater.* 2005; 17:5712–5719.
23. Durandetti M, Devaud M, Perichon J. *New J. Chem.* 1996; 20:659.
24. Budnikova YH, Perichon J, Yakhvarov DG, Kargin YM, Sinyashin OG. *J. Organomet. Chem.* 2001; 630:185–192.
25. Amatore C, Jutand A. *Organometallics*. 1988; 7:2203–2214.

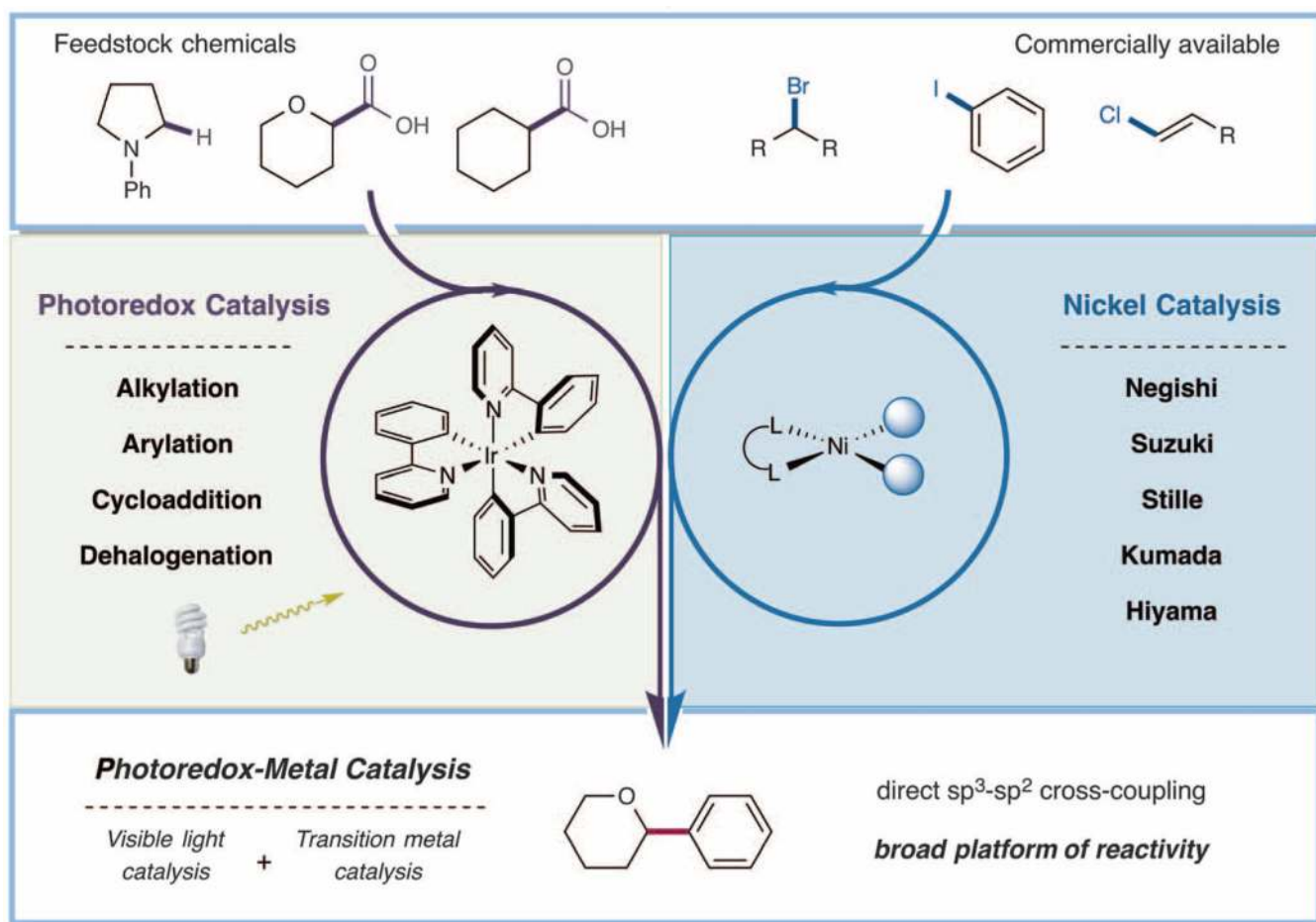


Fig. 1. The merger of photoredox and nickel catalysis yields access to direct sp^3 - sp^2 cross-coupling
R, alkyl group.

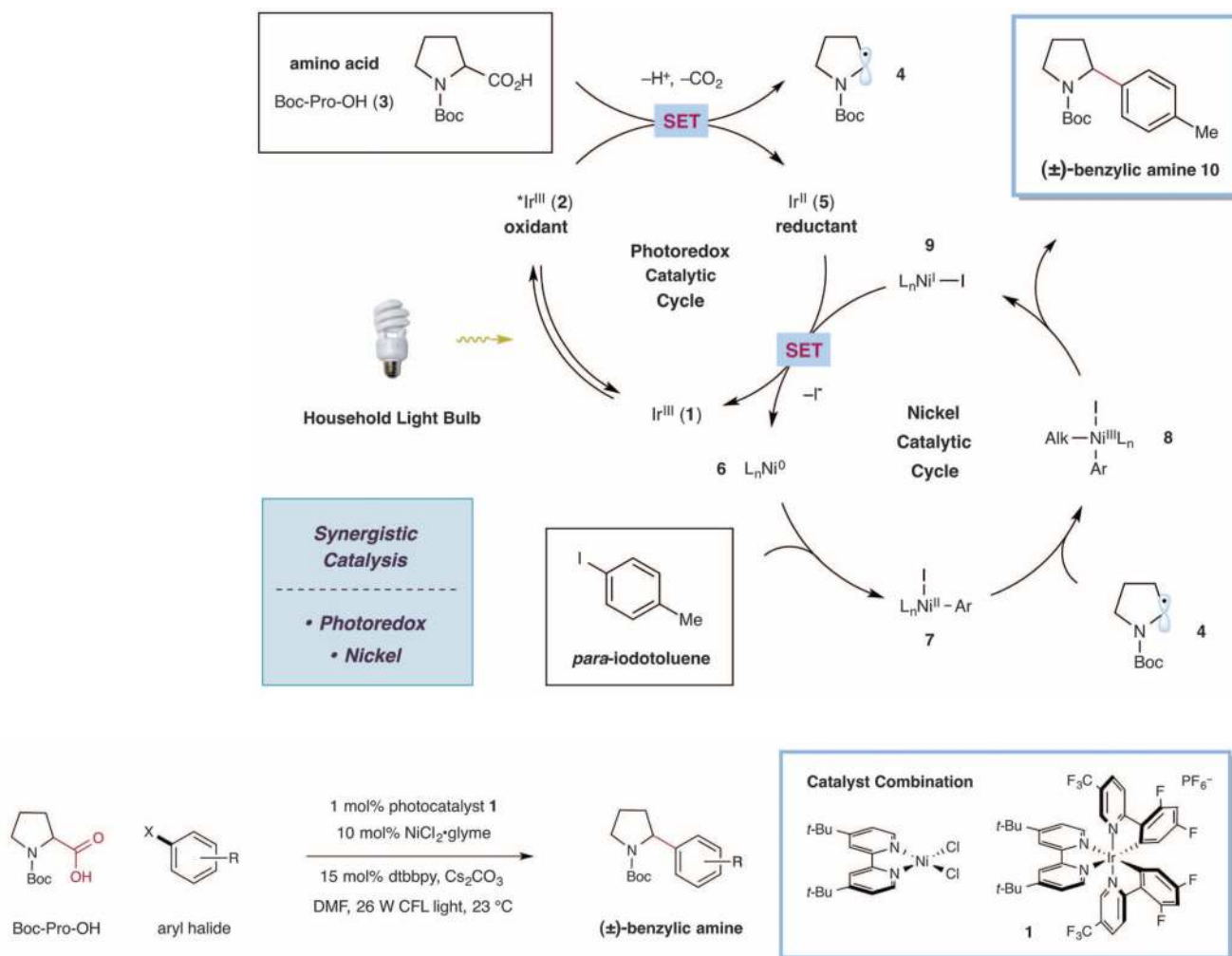


Fig. 2. Proposed mechanistic pathway of photoredox-nickel-catalyzed decarboxylative arylation
Me, methyl group; L, ligand; Alk, alkyl group.

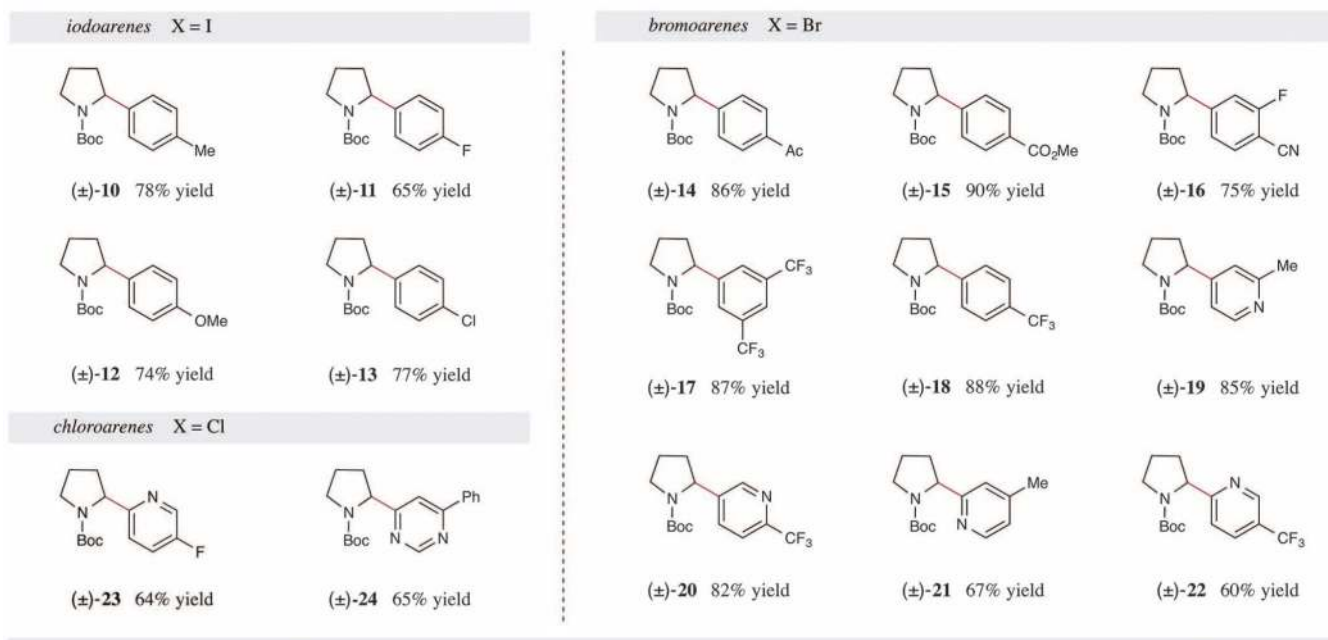


Fig. 3. Photoredox-nickel catalyzed decarboxylative cross-coupling: aryl halide scope
CFL, compact fluorescent light; Bu, butyl group; Ac, acetyl group.

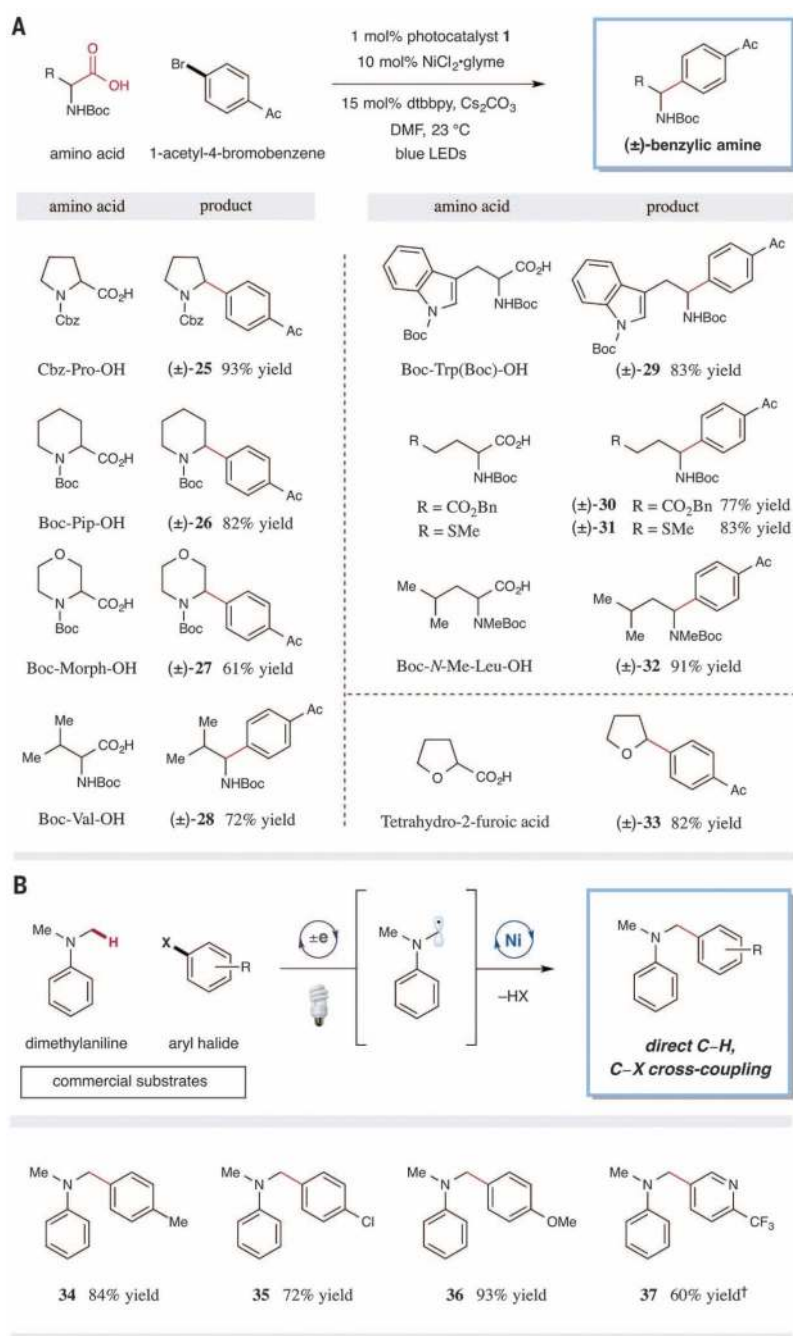


Fig. 4. Amino acid coupling partners and C_{sp}³-H, C-X cross-coupling

(A) Evaluation of the amino acid coupling partner in the decarboxylative-arylation protocol. Ac, acetyl group; LED, light-emitting diode. (B) The direct C_{sp}³-H, C-X cross-coupling via photoredox-nickel catalysis. All yields listed in Figs. 3 and 4 are isolated yields. Reaction conditions for (A) are the same as in Fig. 3. Reaction conditions for (B) are as follows: photocatalyst **1** [1 mole % (mol %)]; NiCl₂·glyme (10 mol %), dtbbpy (15 mol %), KOH (3

equiv.), DMF, 23°C, 26-W light. *Iodoarenes used as aryl halide, X = I. †Bromoarene used, X = Br.